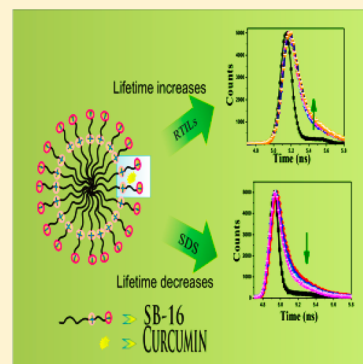


Exploring the Photophysics of Curcumin in Zwitterionic Micellar System: An Approach to Control ESIPT Process in the Presence of Room Temperature Ionic Liquids (RTILs) and Anionic Surfactant

Chiranjib Banerjee, Surajit Ghosh, Sarthak Mandal, Jagannath Kuchlyan, Niloy Kundu, and Nilmoni Sarkar*

Department of Chemistry, Indian Institute of Technology, Kharagpur 721302, West Bengal, India

ABSTRACT: In this manuscript, we have modulated the photophysical properties of curcumin in a zwitterionic (*N*-hexadecyl-*N,N*-dimethylammonio-1-propanesulfonate (SB-16)) micellar aggregates with addition of room temperature ionic liquids (RTILs) as well as commonly used anionic surfactant (SDS), using steady-state and time-resolved spectroscopic techniques. To modulate the photophysics, first we studied its interaction with an SB-16 micellar system, then to further exploit its photophysics, three RTILs (EmimES, EmimBS, EmimHS) with variation of alkyl chain lengths as well as SDS were used. It is observed that the rate of degradation of curcumin is drastically decreased after partitioning into the zwitterionic micellar system. It is shown that the dynamics of excited state intramolecular proton transfer (ESIPT) processes can be controlled by using those RTILs and SDS. Our study also reveals that the hindrance of nonradiative processes of curcumin, i.e., ESIPT is more pronounced in the case of RTIL containing a long alkyl chain compared to a small one. However, most interestingly the addition of long chain (dodecyl) anionic surfactant (SDS) promotes the ESIPT process of curcumin. We have also studied the effect of the addition of inorganic salt and compared the results with RTILs. The present work demonstrates an effort to decipher the photophysics of curcumin in zwitterionic micellar systems by monitoring its excited state dynamics.



1. INTRODUCTION

Medicines derived from plants play an important role in the healthcare of both ancient and modern cultures.^{1,2} Curcumin extracted from the rhizome of turmeric with the structural name 1,7-bis(4-hydroxy-3-methoxyphenyl)-1,6-heptadiene-3,5-dione is a yellow natural pigment with famous use in cosmetics and medicine.^{3,4} At present, curcumin draws much attention due to its numerous pharmacological activities such as anti-inflammatory, antitumor, antioxidant, and other desirable medicinal benefits.^{5–8}

In spite of various advantages, the problem associated with curcumin is its reduced bioavailability.⁹ The low bioavailability of curcumin can be understood by considering its poor water solubility, which makes curcumin difficult to absorb.¹⁰ The lack of stability of curcumin at physiological pH could be due to the presence of seven-carbon β -diketone linker which is susceptible to hydrolysis. As a result, understanding the photophysics of curcumin is required to explore its potential application in medicine.

After analyzing the crystal structure of curcumin, the existence of the keto–enol form has been established.^{11,12} According to Sun et al., among all the possible isomeric structures of curcumin, only three of them have been considered to be present; those are shown in Scheme 1.¹³ Considering the recent literature, one can conclude that the cis-diketo form could be the commonly used representation of curcumin.^{14,15} The existence of the enolic form with extended

resonance between the two phenolic rings is also supported by theoretical results.^{16–18}

There is currently renewed interest in monitoring the singlet and triplet state dynamics of drug molecules.^{19–21} Recent studies of curcumin in various neat solvents,^{22–28} micelles,²⁹ and vesicles³⁰ elucidates the fact that the fastest nonradiative decay kinetics of curcumin proceeds through an excited state intramolecular proton transfer (ESIPT) between the hydroxyl group and the keto group of curcumin followed by radiationless excited-tautomer decay in closed cis-enol tautomer. Very recent, Huppert and co-workers, after performing the temperature dependent experiment, concluded that the solvent controlled proton transfer is the main nonradiative process operating in the excited state.³¹ The effect of addition of mild base on curcumin has also been performed by the same group, who ended up with their previous conclusion.³²

The self-assemblies of surfactants, bile salts, and nanocavities of cyclodextrin are commonly used in the drug industry to control the drug release and uptake, and most importantly to enhance aqueous solubility of the drug.^{33–36} To get a comprehensive idea it is also essential to understand the interaction of curcumin with other biologically resembling assemblies. Petrich and co-workers showed that aggregation of neutral (TX-100), anionic (SDS), and cationic (CTAB)

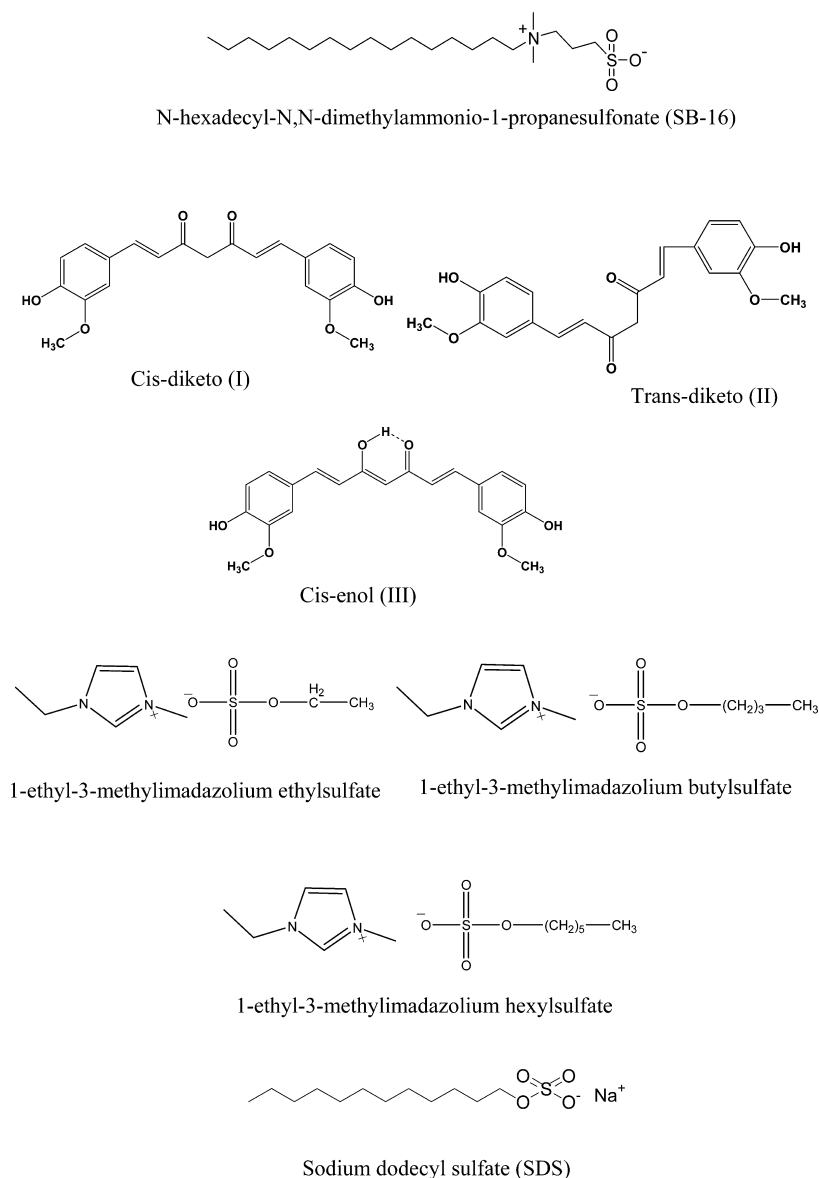
Received: December 1, 2013

Revised: March 11, 2014

Published: March 11, 2014



Scheme 1



surfactants can provide the desirable stability and solubility of curcumin.³⁷ Curcumin is very unstable at elevated pH of the medium, which is often required in medicinal chemistry. Kee and co-workers showed that cationic micelle has the ability to resolve that issue.³⁸ Curcumin in liposomes,³⁹ solid lipid microparticles, such as bovine serum albumin,^{40,41} and chitosan,⁴² or complexed with phospholipids⁴³ and cyclodextrin⁴⁴ has also been reported in literature.

It is very difficult to change the physiochemical properties of a surfactant after a certain concentration other than changing temperature and pressure. One most commonly used technique is to use external additives, such as cosurfactants, cosolvents, nonpolar organics, polar organics, or electrolytes. Room temperature ionic liquids (RTILs) can also play a similar role to modulate the properties of surfactants due to their strange properties.^{45–47} They are environmentally friendly, nontoxic liquids, having melting points below room temperature.⁴⁸ The aggregation number as well as the critical micelle concentration (CMC) can be modulated by using RTILs as external additives.^{49,50} The effectiveness of this modification depends

on various factors among which the most important is extent of interaction between cation/anion of the IL and the headgroup of the surfactant, as well as the hydrophobic interaction of the tail part of both RTIL and surfactant.^{50–53} Recently, Pandey et al. demonstrated the effect of addition of RTILs on a fixed concentration of surfactant.^{54,55} RTILs having longer alkyl chain length can act as cosurfactants and cosolvents as well, depending upon the concentration.

The present aim of this article is to establish the photophysics of curcumin in a milieu having unique polarity, rigidity, as well as morphology. Keeping these in mind, we have modulated the photophysical properties of curcumin in zwitterionic micellar system with addition of RTILs (EmimES, EmimBS, and EmimHS), salt, as well as a commercially available surfactant like SDS. Moreover, by applying our spectroscopic techniques we are also able to show that ESIPT of curcumin can be controlled with these external additives.

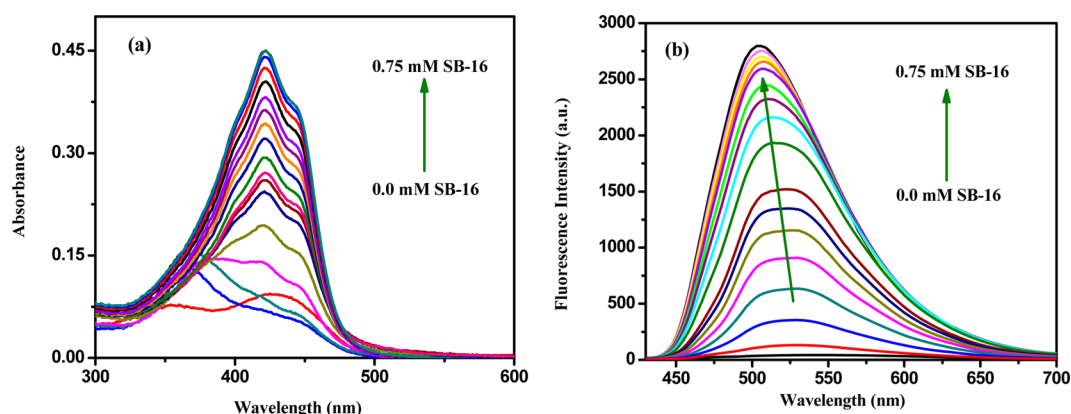


Figure 1. Absorption (a) and emission (b) spectra of curcumin with increasing concentration of SB-16 at 298 K.

2. EXPERIMENTAL SECTION

2.1. Materials. We bought the curcumin from Sigma Aldrich (purity ~81%). The absorption and fluorescence spectra obtained for curcumin are similar to the data presented in the literature, where the purity of the sample was ~99%.¹⁴ Hence we can expect that the 19% mass ratio for the unknown compound could not have any effect on fluorescence properties of curcumin. Both surfactants SDS and SB-16 were procured from Sigma-Aldrich. EmimEs (1-ethyl-3-methylimidazolium ethylsulfate), EmimBs (1-ethyl-3-methylimidazolium butylsulfate), and EmimHs (1-ethyl-3-methylimidazolium hexylsulfate) were purchased from Solvent Innovation GmbH and also used as received (>99% purity). We used Milli-Q water throughout all the experiments. We kept the concentration of curcumin at 2.5×10^{-6} M to measure all the experimental data, and the temperature was 298 K.

2.2. Instruments and Methods. Shimadzu (model no. UV-2450) spectrophotometer and Hitachi (model no. F-7000) spectrofluorimeter are used to measure the absorption and fluorescence spectra. The steady-state anisotropy measurement was performed using a Horiba Jobin Yvon spectrofluorimeter (Fluoromax 4) using a 1 cm quartz cell. One can define steady state anisotropy as⁵⁶

$$r_0 = \frac{I_{VV} - G \cdot I_{VH}}{I_{VV} + 2G \cdot I_{VH}} \quad (1)$$

where G is the correction factor. I_{VV} and I_{VH} are the emission intensities of the sample with one case when both excitation polarizer and emission polarizer are oriented vertically, another case when excitation polarizer is oriented vertically and the emission polarizer is horizontally oriented. Measurement of fluorescence lifetimes was performed using a time-correlated single photon counting (TCSPC) spectrometer of IBH (U.K.). The details of our experimental setup is described in our earlier publication.⁵⁷ However, it is also necessary to describe in brief; upon excitation of the sample with a laser diode we have collected the signal at a magic angle of 54.7° using a Hamamatsu microchannel plate photomultiplier tube (3809U). The instrument response function is also an important function to determine the lifetime more accurately, which was ~90 ps.

The average lifetimes of curcumin were calculated after fitting the decay curve with a biexponential fit. Equation 2 is applied to determine the average lifetime.⁵⁶

$$\tau_{av} = a_1\tau_1 + a_2\tau_2 \quad (2)$$

where τ_1 and τ_2 are the first and second lifetime components that were monitored at the emission maxima and a_1 and a_2 are the corresponding weights of those components.

The quantum yield of the curcumin was calculated by applying the commonly used eq 3⁵⁶

$$\frac{\Phi_S}{\Phi_R} = \frac{A_S}{A_R} \times \frac{(Abs)_R}{(Abs)_S} \times \frac{n_S^2}{n_R^2} \quad (3)$$

In eq 3 Abs stands for absorbance, Φ represents quantum yield, and the subscripts S and R represent the corresponding parameters for the sample (curcumin) and reference (coumarin 153), respectively. n is the refractive index of the medium, and A corresponds to the area under the fluorescence curve. The subscripts S and R represent the corresponding parameters for the sample (curcumin) and reference (coumarin 153), respectively. The quantum yield (Φ) of curcumin was determined by considering the reported Φ of C153 in acetonitrile which is 0.56.⁵⁸

3. RESULTS AND DISCUSSION

3.1. Steady-State Absorption and Emission Studies.

The spectral properties of curcumin in SB-16 micelle and upon addition of RTILs (EmimEs, EmimBs, EmimHs), as well as long chain surfactant (SDS), were studied systematically to investigate the photophysics in these confined media. Curcumin absorbs visible light and gives fluorescence with very low quantum yield. In water curcumin shows an intense absorption band at 430 nm with another band at 355 nm. The absorption band corresponding to 430 nm is ascribed to the lowest ($\pi-\pi^*$) transitions present in the conjugated curcumin and the shoulder peak at 355 nm is associated with the $\pi-\pi^*$ transitions in the feruloyl unit.^{59,60} Now, with addition of a zwitterionic surfactant (SB-16) at very low concentration, the absorbance of the peak at 430 nm decreases and becomes a broad shoulder, while the shoulder at 355 nm transfers to a clear peak. Another notable observation is that the newly generated absorption peak at 355 nm at that concentration is somewhat red-shifted. However, at higher concentration of SB-16 (0.75 mM), the peak at 355 nm decreases in intensity and changes to a shoulder again, whereas the absorption peak at 430 nm is enhanced and finally shifted to a peak at 421 nm with shoulder at 443 nm. The reversal of the absorption spectrum of curcumin at higher and lower concentrations of SB-16 can be attributed to two different types of interactions occurring: increasing hydrophobic interaction between the hydrophobic aryl groups of curcumin and SB-16 micelle at higher

concentration of SB-16, and electrostatic interaction between charged headgroup of SB-16 with the β -diketone group of curcumin to form SB16–curcumin complexes at lower concentration. The absence of the peak at 355 nm and the 9 nm blue shift of the 430 nm peak is a signature of the movement of the curcumin from bulk water to the micellar environment. Similar types of absorption peaks in TX-100, DTAB, and SDS are reported in the literature.³⁷ However, in the case of SDS micelle, the shoulder peak at 443 nm is absent in the absorption spectrum. The above information reveals that the curcumin is located inside the palisade layer of the zwitterionic micelle. The absorption spectra of curcumin with gradual increase of SB-16 are depicted in Figure 1a.

To monitor the excited state dynamics (S_1) of curcumin it is essential to record the emission spectra also.⁶¹ Curcumin in aqueous solution exhibits a broad emission spectrum with low fluorescence intensity. However, with a gradual increase in the concentration of SB-16 the fluorescence intensity of curcumin increases considerably. The increase in fluorescence intensity is accompanied by the gradual blue shift in emission maximum, which finally saturates at 502 nm with the addition of 0.75 mM SB-16. The 48 nm blue shift implies the movement of curcumin toward the micellar aggregates from bulk water. The emission spectrum of curcumin shows a broad spectrum peaked at 498, 501, and 548 nm in the DTAB, TX-100, and SDS micelles, respectively;³⁷ hence, the microenvironment sensed by the curcumin in zwitterionic surfactant is nearly similar to the TX-100 micelle. Encapsulation of drug molecules into the micelle can render the drug completely dispersible in water, making the drug intravenously injectable. Biodegradable polymeric nanoparticles are viewed as excellent candidates for anticancer drug delivery systems,^{62,63} and some biodegradable polymer nanoparticle-delivered anticancer drugs are already on the market.⁶⁴ The photophysical study of curcumin in our present system, i.e., zwitterionic micellar aggregates, can provide insight into such unprecedented systems mentioned above.

3.2. Determination of Partition Coefficient. The significant spectral changes in the corresponding absorption and fluorescence spectra of curcumin in micellar solution compared to the bulk water may be due to the interaction of curcumin with zwitterionic surfactant (SB-16). The change in the spectral property reflects significant partitioning of curcumin into the palisade region of micellar aggregates. Hence it is essential to have an idea about the level of penetration of curcumin with the addition of SB-16. To determine the partition constant it is essential for only one curcumin to be present per micelle; hence, we kept the concentrations of SB-16 in the millimolar range. The partition coefficient of a curcumin between bulk water and micellar system can be determined as follows:⁶⁵

$$K_p = \frac{(C_m/C_t)/[\text{SB-16}]}{(C_w/C_t)/[\text{Water}]} \quad (4)$$

where C_t is the total concentration of curcumin; C_w and C_m are related to the probe concentrations in water and micellar aggregates, respectively. However, for experimental purposes it is easy to determine the partition coefficient from the fluorescence spectra of probe molecules with increasing amount of surfactant concentration. The required equation is given below:

$$\frac{I_\infty - I_0}{I_t - I_0} = 1 + \frac{[\text{Water}]}{K_p} \times \frac{1}{[\text{SB-16}]} \quad (5)$$

In the above expression I_0 , I_t , and I_∞ are the emission intensities of the curcumin in bulk water, at different concentrations of surfactant above the CMC, and at a condition when the fluorescence intensity becomes saturated. K_p is the partition coefficient of curcumin to the zwitterionic micellar aggregates from the pure water. Figure 2 represents linear plots of $(I_\infty -$

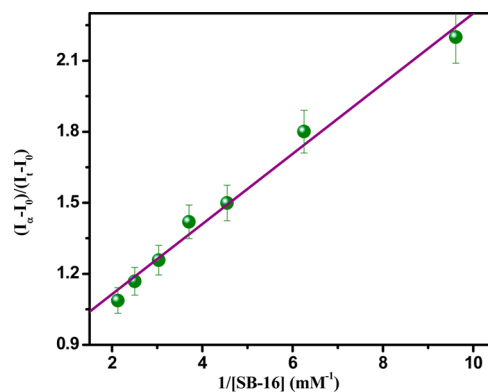


Figure 2. Plot of $(I_\infty - I_0)/(I_t - I_0)$ vs $[\text{SB-16}]^{-1}$ for determination of the partition coefficient.

$I_0)/(I_t - I_0)$ versus $[\text{SB-16}]^{-1}$ for determination of the partition function. From the slope of the eq 5 the partition coefficient has been calculated. Analysis of the result discloses the fact that the curcumin exhibits a quite high partition coefficient for zwitterionic micellar aggregates; the calculated value is 15×10^4 . The significant partitioning of curcumin inside the zwitterionic micelle implies higher stability of the drug inside the investigated micellar system.

3.3. Determination of Steady State Anisotropy (r_0).

The rigidity of the microenvironment can be understood by measuring the steady-state anisotropy of our investigated drug molecules, as polarization (anisotropy) measurements can reveal the details about the binding phenomenon. From the changes occurring in the steady state anisotropy value upon addition of surfactant, one can get fruitful information about the microenvironment around the probe molecules.^{66–70} We have determined the steady state fluorescence anisotropies (r_0) with increasing concentration of SB-16 in a solution of curcumin. The anisotropy value with variation of SB-16 is shown in Figure 3: it is clear that with the addition of SB-16 in a solution of curcumin the anisotropy value increases up to certain limit, and it is independent of concentration afterward. The increase in anisotropy value with gradual increase of SB-16 is a manifestation of the transfer of the probe molecule from the bulk water to the micellar aggregates. Moreover, with increasing concentration of SB-16 the fluorophore experiences a confined environment with respect to that in bulk water. The experimental anisotropy value at the saturation level is 0.307, which is quite high and comparable with our previous study.⁷⁰ The significantly higher anisotropy value of curcumin at the saturation level can be understood by considering the rigidity of the micellar aggregates.

3.4. Determination of Binding Constant (K_b). In order to determine the extent of intermolecular binding between curcumin and zwitterionic micelles, we measured the binding constant (K_b). Generally speaking, the binding of drug in

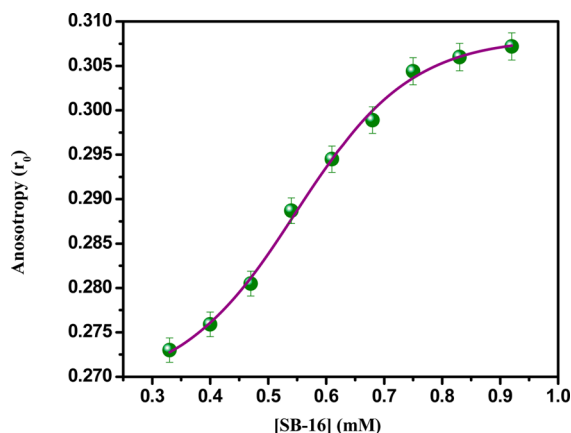


Figure 3. Change of steady-state fluorescence anisotropy of curcumin with increasing concentration of SB-16.

organized assembly is a basic and important process in solution chemistry. Due to the modulation of the physical and chemical processes, an organized micellar system may prevent the external perturbation in solution. To determine the binding constant between curcumin and SB-16 micelle, we followed the method described by Almgren et al.⁷¹ The general equation to determine the binding constant is given below:

$$\frac{I_{\infty} - I_0}{I_t - I_0} = 1 + \frac{1}{K_b[M]} \quad (6)$$

where I_0 is the emission intensity of curcumin in the absence of SB-16, I_t is the emission intensity at each and every intermediate concentration, and I_{∞} is the emission intensity of curcumin at a condition of saturation, respectively, and K_b is the binding constant between curcumin and SB-16 micellar system. $[M]$ could be described in the following way:

$$[M] = \frac{[\text{SB-16}] - \text{CMC}}{N_{\text{agg}}}$$

where $[\text{SB-16}]$ describes the micellar concentration and N_{agg} describes the aggregation number of the micellar system. CMC is the critical micellar concentration, i.e., the concentration at which SB-16 starts to aggregate to form micelle. Variation in $(I_{\infty} - I_0)/(I_t - I_0)$ versus $[M]^{-1}$ from eq 6 gives a linear plot from which we have determined the binding constant (K_b). The value we obtained from Figure 4 was $5 \times 10^4 \text{ M}^{-1}$ for the

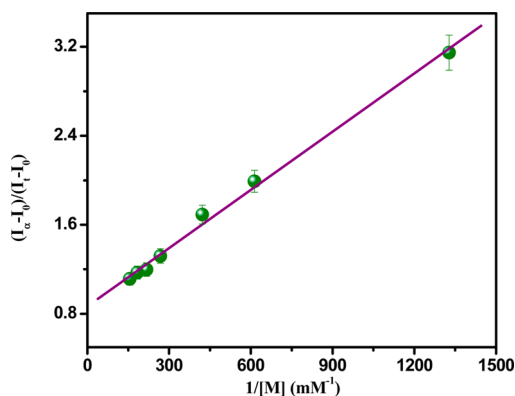


Figure 4. Plot of $(I_{\infty} - I_0)/(I_t - I_0)$ vs $[M]^{-1}$ for the determination of binding constant.

binding constant. The large value of binding constant supports the favorable interaction between the drug and micellar aggregates. Such a high value of binding constant may be due to the formation of hydrogen bonding between the negatively charged sulfonate group of SB-16 and free hydroxyl groups of curcumin. In our earlier publication we also reported a similar type of hydrogen bonding between the negatively charged sulfonate group of AOT and free hydroxyl groups of curcumin,⁷⁰ although we cannot ignore the possibility of van der Waals interaction between the hydrophobic chain of SB-16 micelle and two phenyl moieties of curcumin.

3.5. Effect of RTILs and Surfactant. We have also observed some interesting phenomena associated with our investigated system, such as the effects of RTILs and anionic surfactant on the drug–micellar aggregates. The main aim in this comparative study is to see the effect of alkyl chain of RTILs and SDS. At first, curcumin was taken in water and the required amount of SB-16 was added to get saturation in fluorescence intensity. In our experimental condition the concentration of SB-16 was kept at 0.75 mM. In our previous study we determined the CMC as well as aggregation number of SB-16, which were $0.096 \pm 0.005 \text{ mM}$ and 81 ± 8 , respectively.⁵¹ However, in the present article we performed all the experiments at 0.75 mM SB-16, as the fluorescence intensity saturates at this concentration. To study the effect of RTILs on zwitterionic micellar systems, we first added an RTIL with small alkyl chain, i.e., EmimES, to SB-16 micelle. It was found that the fluorescence intensity of curcumin starts to increase with increasing concentration of EmimES and becomes saturated up to the addition of 1.96 wt % of EmimES. To clarify the effect of EmimES we also added two other RTILs, i.e., EmimBS and EmimHS, which had similar observations, i.e., fluorescence intensity of curcumin increased with increasing concentration of EmimBS and EmimHS (Figure 5). On close inspection of the results, we found that the effect of the addition of RTILs is more pronounced for the one having longer alkyl chain, i.e., EmimHS. This can be inferred from the fact that the three RTILs act as electrolytes which decrease the CMC of SB-16 micelle and follow the order EmimHS > EmimBS > EmimES.⁵¹ In the case of EmimHS, in the presence of longer alkyl chain (hexyl chain) the hydrophobic interaction with SB-16 micelle is more comparable to EmimES, consisting of a very small chain (ethyl chain). Hence, the difference behavior is due to the different chain length of RTILs. When the CMC of SB-16 decreases, the partitioning of the curcumin into the zwitterionic micelle increases compared to the system where the CMC is higher; as a result, the fluorescence intensity increases. The higher fluorescence intensity could be mainly two reasons: the first one is higher solubility and stability in the micellar system, and the second one is the perturbation of the ESIPT process, which is properly taken care of in the time-resolved part. To further support this phenomenon we also studied the photophysics of curcumin with the addition of salt (sodium chloride, NaCl). A monotonic increase of the emission spectrum of curcumin is observed with increasing concentration of NaCl to the SB-16 micellar solution, implying the similarity to RTILs (Figure 5d). Another important observation is that at very high concentration of RTILs the fluorescence intensity of curcumin decreases. The increase in CMC at higher concentrations of RTILs can be attributed to the fact that EmimES, EmimBS, and EmimHS act as cosolvents at higher concentrations, and low solvophobicity between the RTILs and the hydrophobic tail of

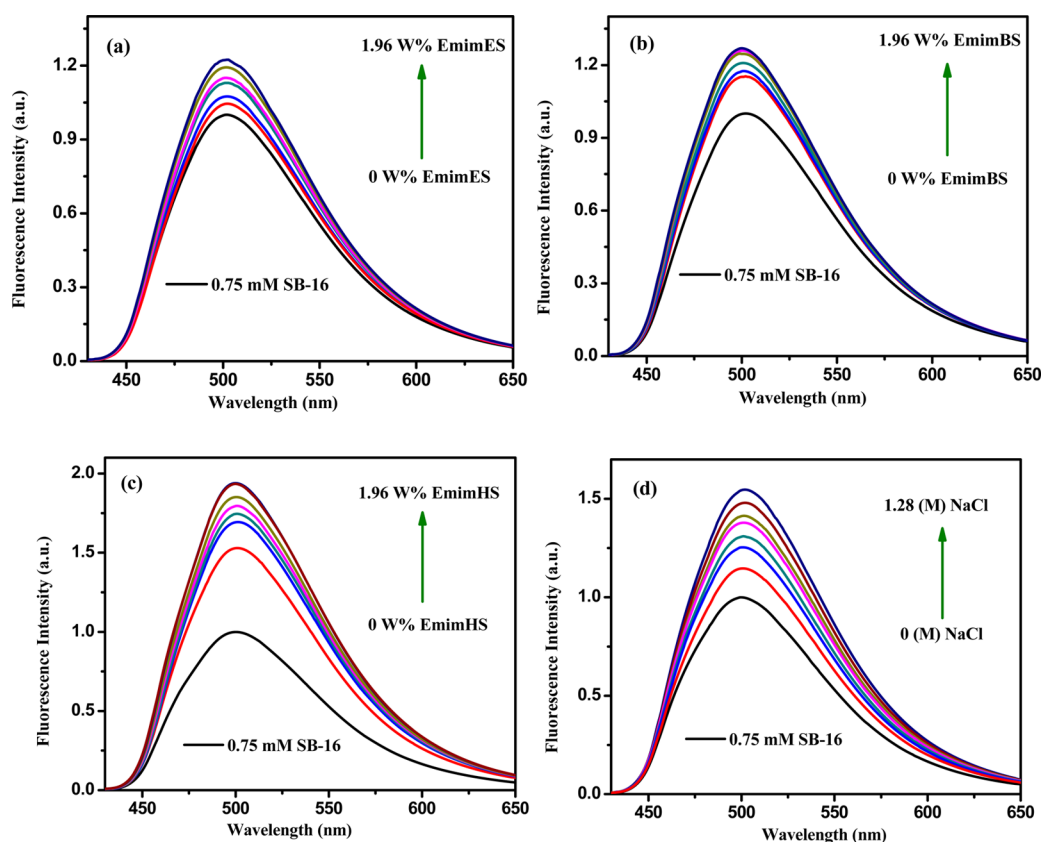


Figure 5. Fluorescence spectra of curcumin in SB-16 micellar system with addition of (a) EmimES, (b) EmimBS, (c) EmimHS, and (d) NaCl.

the surfactant molecule leads to a high CMC.⁵¹ As a result, the percentage of curcumin molecules entering into the palisade layer of the micelles decreases.

Hence we can conclude that the increase in fluorescence intensity which is observed with the addition of RTILs may be due to the decrease in CMC of SB-16 micellar solution. Although we cannot ignore the other fact that, due to the hydrophobic interaction of alkyl (hexyl) chain of RTILs with the long tail of SB-16, the possibility of hydrogen bonding between curcumin and sulfonate group attached to the alkyl chain of the RTILs increases, i.e., ESIPT of curcumin decreases, leading to an enhancement of fluorescence intensity. However, the effect of the addition of long chain anionic surfactant (SDS) is completely reversed with respect to RTILs. With gradual addition of SDS from 7.83 mM to 14.14 mM, the fluorescence intensity of curcumin drastically decreases along with ~ 20 nm red shift, implying movement of the probe molecules from the palisade layer of the zwitterionic micellar system (SB-16) to bulk water (Figure 6). The movement of the probe molecule can be ascribed to the presence of the long alkyl (dodecyl) chain on SDS, which can easily orient itself and fuse inside the SB-16 micelle, increasing the hydration of the palisade layer of the zwitterionic micellar system according our previous study.⁵² However, a similar fusion process is difficult in the case of RTILs due to the short alkyl (ethyl, butyl, and hexyl) chain (Scheme 2). Increasing hydration of the micellar palisade layer facilitates the ESIPT process of curcumin leading to a decrease in fluorescence intensity. Time resolved experiments also support the above incident (vide infra).

3.6. Degradation Study. The solubility of curcumin is very poor in water at neutral or acidic pH. The compound is, however, soluble in alkaline pH. The reported pH values for the

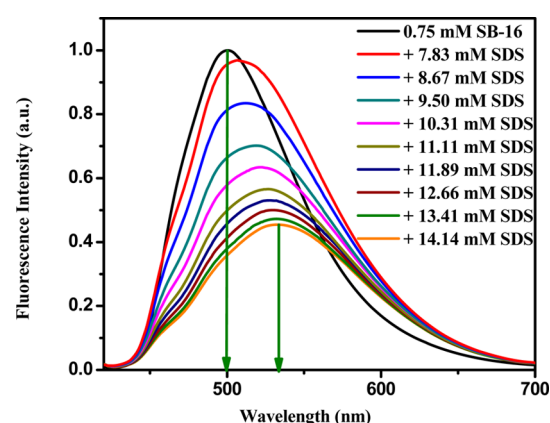
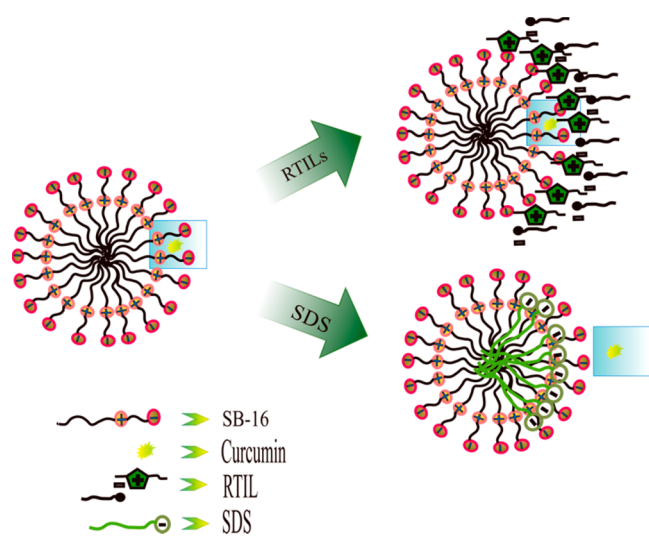


Figure 6. Fluorescence spectra of curcumin in SB-16 micellar system with addition of anionic surfactant (SDS).

dissociation of the three acidic protons in curcumin are 8.31, 10.0, and 10.2, respectively.³⁸ Due to the instability of β -diketone linker in curcumin, it dissociates to vanillin, ferulic acid, and feruloyl methane leading to decrease in absorbance value.⁶⁵ The 80% degradation of curcumin is reported in aqueous buffer (pH 7.4) solution after 1 h of interval.⁷² In our present study, we have investigated the stability of curcumin in zwitterionic micellar system in absence and presence of RTIL. The extent of degradation of curcumin in our studied systems has been determined by monitoring the time-dependent absorption spectra. The time-dependent absorption spectra of curcumin in SB-16 micelle in the absence and presence of EmimHS have been shown in Figure 7a and b, respectively. Our results reveal that zwitterionic micellar assemblies

Scheme 2



significantly reduce the degradation rate (percentage of degradation <5% after 12 h) of curcumin due to partitioning into the palisade layer of zwitterionic micelles from bulk water. It is also observed that the rate of degradation of curcumin is almost the same in the presence of EmimHS. The higher stability of curcumin in these organized assemblies at neutral pH could be due to the reduced interaction with bulk water. A similar degradation rate is reported on binding with hydrophobic cavities of cyclodextrins and proteins.^{72–74} Our previous report, where we studied the stability of curcumin in niosome, also showed higher stability of curcumin (the degradation rate was <20% after 12 h).⁷⁵ Quin et al. very recently showed that upon encapsulation into monomethoxy poly(ethylene glycol)-poly(3-caprolactone) (MPEG-PCL) micelles the stability of curcumin greatly improved.⁷⁶ Moreover, they also demonstrated that the efficiency of intravenous application of curcumin loaded micelles drastically improved compared to that of free curcumin. From this point of view, i.e., very high stability of curcumin, the zwitterionic micellar system may serve as a good model system to study its medicinal effect.

3.7. Effect of Temperature. The major interaction forces between small organic molecules and biological macromolecules are electrostatic interactions, hydrophobic forces, van der Waals force, and hydrogen bonding interactions.⁷⁷ The

thermodynamic rules to estimate the type of binding interaction between a biological macromolecule and an organic micromolecule are reported by Ross et al.⁷⁸ We have determined the nature of interaction between SB-16 and curcumin using the thermodynamic parameters. With elevation of temperature from 10 to 60 °C at a fixed concentration (0.75 mM) of SB-16, the fluorescence intensity of curcumin gradually decreases (Figure 8). The change in entropy (ΔS) and enthalpy

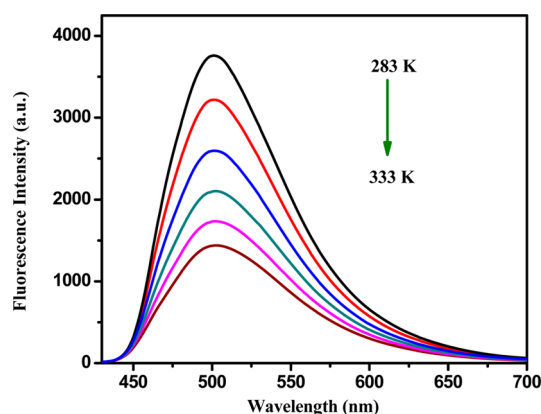


Figure 8. Fluorescence spectra of curcumin in SB-16 with variation of temperature.

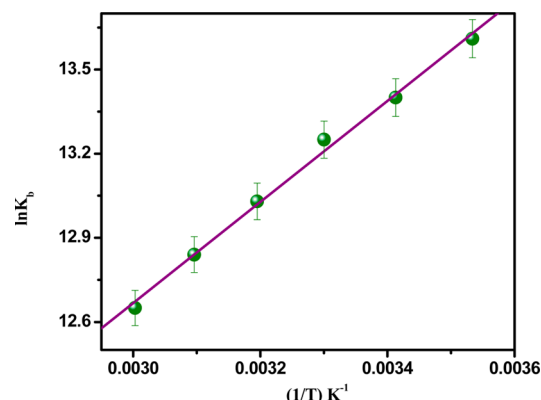


Figure 9. van't Hoff plot of curcumin in SB-16 micelle at different temperatures.

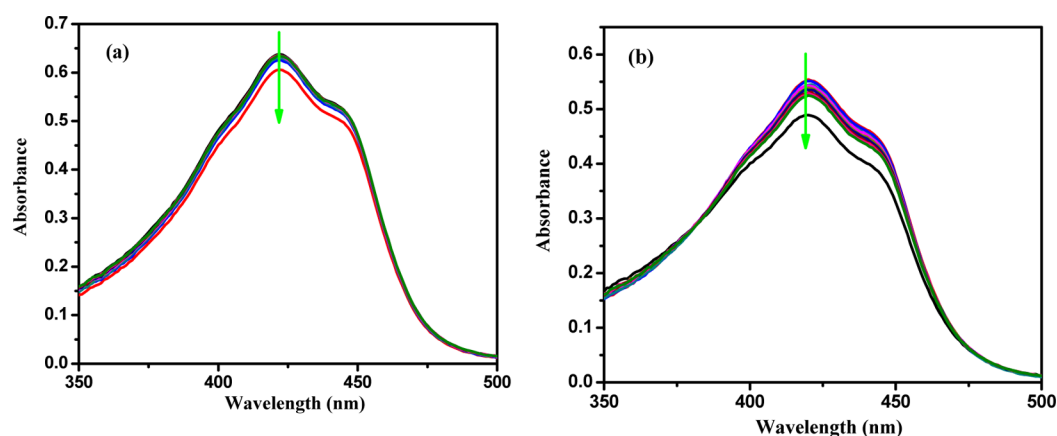


Figure 7. Changes in the absorption spectra of curcumin in (a) SB-16 micelle and (b) EmimHS-SB16 micelle with increasing time.

(ΔH) can be measured by plotting $\ln K_b$ vs $1/T$ (Figure 9) applying van't Hoff equation [$\ln K_b = (-\Delta H/R)/T + \Delta S/R$]. It is also possible to determine the Gibbs free energy by applying the equation $\Delta G = -RT \ln K_b$, where R is the universal gas constant and T is the absolute temperature (Table 1).

Table 1. Change in Binding Constant and Free Energy (ΔG) at Different Temperatures^a

temperature (K) (Curcumin in 0.75 mM SB-16)	$K_b \times 10^5$ (M^{-1})	$\ln K_b$	$-\Delta G$ (kcal/mol)
283	8.18	13.61	7.70
293	6.64	13.40	7.85
303	5.73	13.25	8.03
313	4.58	13.03	8.15
323	3.77	12.84	8.29
333	3.13	12.65	8.42

^a ΔH (kcal/mol) = -3.61 and ΔS (cal/mol) = 14.48 in this temperature range.

The negative value of Gibbs free energy (ΔG) shown in Table 1 indicates the spontaneous nature of interaction between zwitterionic micelle and curcumin. The negative values of ΔH (-3.61 kcal/mol) implying the exothermic nature of interaction and positive value of ΔS (14.48 cal/mol) gives the evidence that the process is entropy driven.

3.8. Time-Resolved Studies. The time-resolved fluorescence profiles of curcumin with addition of SB-16 as well as addition of RTIL and SDS on curcumin–SB16 micelle were

recorded at an emission wavelength of 503 nm upon excitation with a diode laser working at 408 nm. Figure 10a represents the decay profiles of curcumin with addition of SB-16. The lifetime values obtained after biexponential fitting of the fluorescence decay curves are listed in Table 2. One can interpret the location of probe molecules in heterogeneous media after careful analysis of fluorescence lifetime data. The fluorescence lifetime of probe molecules varied for different microheterogeneous system like micelles, reverse micelles, and vesicles. In most of the cases the fluorescence decay profiles obtained from TCSPC setup in organized media as well as in organic solvents show multiexponential fitting, where the lifetime significantly depends on the nature of the media.^{40,79,80} In this case the decay profile of curcumin is found to be biexponential in nature with good χ^2 values (Table 2), which suggests some local heterogeneity in the distribution of the probe, although its location is established to be mostly at the palisade region of the SB-16 micelle. The occurrence of heterogeneity can be attributed to the different modes of interaction of curcumin with SB-16. Due to the complex nature of the interaction it is easy to consider average lifetime of the probe molecules instead of considering each and every component. The average lifetime can be calculated from eq 2.

The decay components of curcumin were assigned mainly due to two processes: ESIPT²⁸ and solvation.^{31,79,80} Palit and co-workers have studied the excited state dynamics of curcumin in different neat solvents by applying absorption spectroscopic and time-resolved fluorescence techniques.¹⁴ In nonpolar solvents, curcumin can easily form a six-membered hydrogen

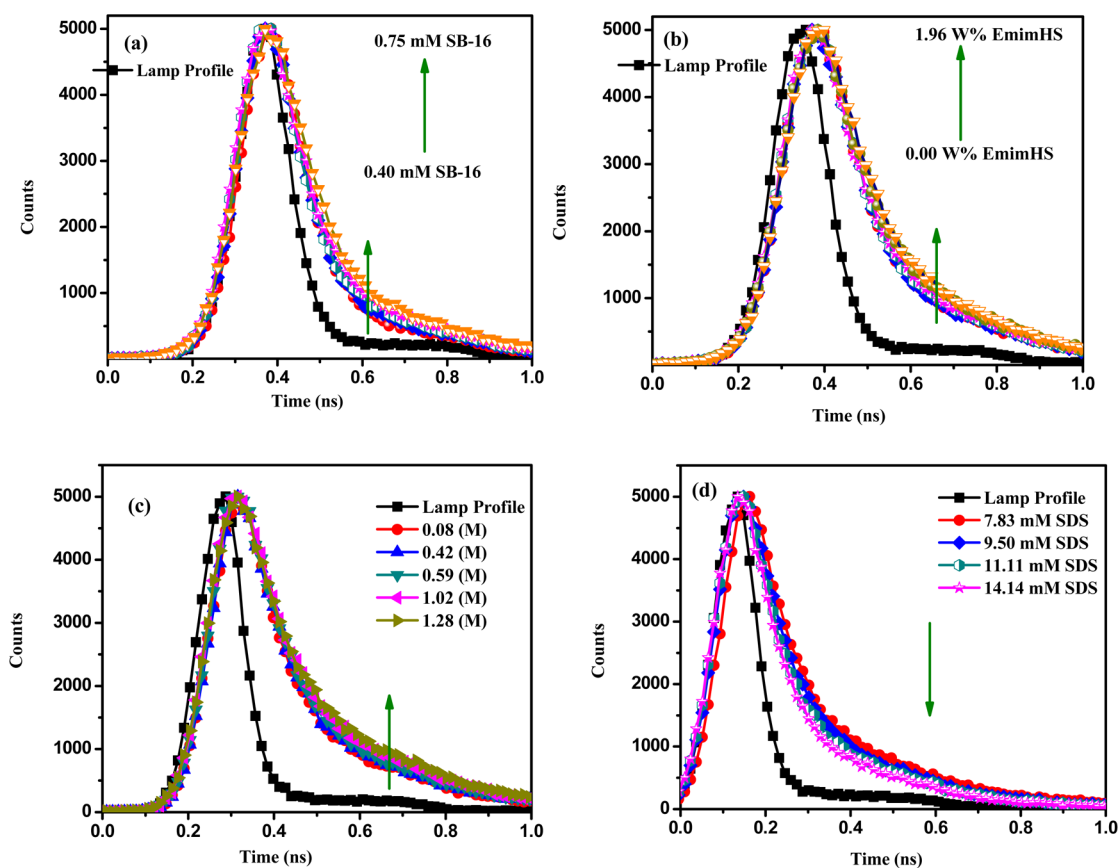


Figure 10. Time-resolved decays of curcumin on (a) addition of SB-16, (b) addition of EmimHS in SB16 micellar system, (c) addition of NaCl, and (d) addition of SDS in SB-16 micellar system.

Table 2. Fluorescence Lifetime, Quantum Yield, Nonradiative Rate and Radiative Rate Constants of Curcumin in SB-16 Micelle at Different Concentrations

systems	τ_1 (a_1)(ps)	τ_2 (a_2)(ps)	$\langle\tau\rangle^a$ (ps)	quantum yield (Φ_x)	K_{nr} (s^{-1}) / 10^9	K_r (s^{-1}) / 10^8
Curcumin in 0.40 mM SB-16	32 (0.80)	137 (0.20)	53	0.017	18.54	3.20
Curcumin in 0.47 mM SB-16	47 (0.78)	157 (0.22)	71	0.020	13.80	2.80
Curcumin in 0.55 mM SB-16	65 (0.76)	161 (0.24)	88	0.020	11.13	2.20
Curcumin in 0.61 mM SB-16	69 (0.80)	184 (0.20)	92	0.025	10.59	2.70
Curcumin in 0.68 mM SB-16	73 (0.79)	194 (0.21)	98	0.029	9.90	2.90
Curcumin in 0.75 mM SB-16	79 (0.84)	236 (0.16)	104	0.032	9.30	3.70

^aExperimental error of $\pm 10\%$.**Table 3. Fluorescence Lifetime, Quantum Yield, Nonradiative Rate, and Radiative Rate Constants of Curcumin in SB-16 Micelle with Addition Different Concentrations of EmimHS**

systems	τ_1 (a_1)(ps)	τ_2 (a_2)(ps)	$\langle\tau\rangle^a$ (ps)	quantum yield (Φ_x)	K_{nr} (s^{-1}) / 10^9	K_r (s^{-1}) / 10^8
Curcumin in 0.75 mM SB-16	79 (0.84)	236 (0.16)	104	0.032	9.30	3.70
+ 0.09 W% EmimHS	77 (0.74)	232 (0.26)	117	0.033	8.26	2.80
+ 0.34 W% EmimHS	85 (0.79)	260 (0.21)	121	0.038	7.95	3.10
+ 0.59 W% EmimHS	87 (0.79)	267 (0.21)	125	0.040	7.68	3.20
+ 0.99 W% EmimHS	90 (0.79)	275 (0.21)	129	0.045	7.40	3.40
+ 1.47 W% EmimHS	95 (0.78)	290 (0.22)	138	0.046	6.91	3.30

^aExperimental error of $\pm 10\%$.**Table 4. Fluorescence Lifetime, Quantum Yield, Nonradiative Rate, and Radiative Rate Constants of Curcumin in SB-16 Micelle with Addition Different Concentrations of NaCl**

systems	τ_1 (a_1)(ps)	τ_2 (a_2)(ps)	$\langle\tau\rangle^a$ (ps)	quantum yield (Φ_x)	K_{nr} (s^{-1}) / 10^9	K_r (s^{-1}) / 10^8
Curcumin in 0.75 mM SB-16	79 (0.84)	236 (0.16)	104	0.032	9.30	3.70
+ 0.42 (M) NaCl	79 (0.80)	244 (0.20)	112	0.035	8.61	3.12
+ 0.59 (M) NaCl	88 (0.79)	255 (0.21)	123	0.038	7.82	3.08
+ 1.02 (M) NaCl	93 (0.76)	266 (0.24)	134	0.039	7.17	2.91
+ 1.28 (M) NaCl	98 (0.77)	270 (0.23)	137	0.043	6.98	3.13

^aExperimental error of $\pm 10\%$.**Table 5. Fluorescence Lifetime, Quantum Yield, Nonradiative Rate, and Radiative Rate Constants of Curcumin in SB-16 Micelle with Addition Different Concentrations of SDS**

systems	τ_1 (a_1)(ps)	τ_2 (a_2)(ps)	$\langle\tau\rangle^a$ (ps)	quantum yield (Φ_x)	K_{nr} (s^{-1}) / 10^9	K_r (s^{-1}) / 10^8
Curcumin in 0.75 mM SB-16	79 (0.84)	236 (0.16)	104	0.032	9.30	3.70
+ 7.83 mM SDS	71 (0.82)	195 (0.18)	93	0.030	10.43	3.20
+ 9.50 mM SDS	64 (0.84)	192 (0.16)	85	0.025	11.47	2.90
+ 11.11 mM SDS	63 (0.87)	189 (0.13)	79	0.021	12.39	2.60
+ 14.14 mM SDS	56 (0.87)	174 (0.13)	71	0.017	13.84	2.40

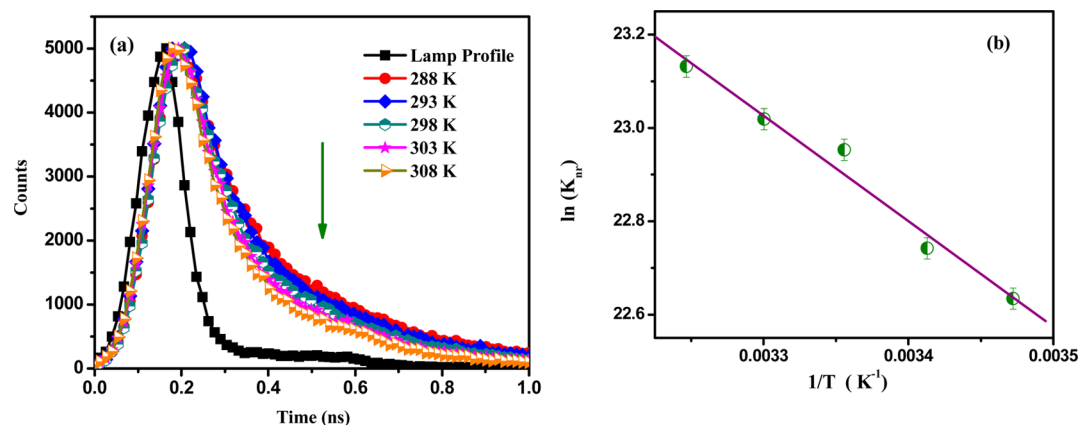
^aExperimental error of $\pm 10\%$.

bonded chelate ring, i.e., ESIPT process drastically increases leading to a very short lifetime of few hundred femtoseconds.⁸¹ However, in polar solvent, like methanol, due to the disruption of ESIPT process the lifetime of curcumin possesses a major component with a lifetime of 130 ps.¹⁴ The similarity between the time constant of ESIPT and the lifetime of fluorescence in the investigated system shows that ESIPT is the main photophysical process to deactivate the excited state of curcumin. In 0.40 mM SB-16 solution, curcumin shows an average lifetime of 53 ps with components 32 (80%) and 137 (20%) ps, which increases with the gradual increase of concentration of SB-16. At the concentration of 0.75 mM it reaches the average value of 104 ps with components 79 (84%) and 236 (16%) ps. The increase of average lifetime with addition of SB-16 (depicted in Table 2) may be attributed to intermolecular hydrogen bonding between the hydroxyl group of curcumin and sulfonate group of SB-16, i.e., hindrance of

ESIPT process is the main responsible factor, although the possibility of van der Waals interaction between the hydrophobic chain of SB-16 micelle and two phenyl moieties of curcumin cannot be ignored. Another important observation is that the amplitude of the each component remains almost constant, which indicates that there is very little effect of hydration on palisade layer of SB-16 micelle. To study the effect of addition of RTILs the measurements of fluorescence lifetime of curcumin with increasing concentration of RTIL on curcumin-SB16 micelle have been performed (Figure 10b). With addition of 1.96 wt % of EmimHS, the average lifetime value of curcumin increased from 104 ps with components 79 (84%) and 236 (16%) to 138 ps with components 95 (0.78%) and 290 (0.22%). The experimental values with intermediate concentrations are listed in Table 3. The increase in lifetime of curcumin with addition of RTILs support our steady state conclusion that at lower concentration they are acting as

Table 6. Fluorescence Lifetime, Quantum Yield, Nonradiative Rate, and Radiative Rate Constants of Curcumin in SB-16 Micelle at Different Temperature

temperature (K)	τ_1 (a_1)(ps)	τ_2 (a_2)(ps)	$\langle\tau\rangle^a$ (ps)	quantum yield (Φ_x)	K_{nr} (s^{-1}) / 10^9	K_r (s^{-1}) / 10^8
288	93 (0.78)	320 (0.22)	142	0.039	6.76	2.70
293	91(0.82)	300 (0.18)	128	0.035	7.53	2.70
298	79 (0.84)	236 (0.16)	104	0.032	9.30	3.00
303	66 (0.79)	222 (0.21)	98	0.026	9.93	2.60
308	65 (0.84)	210 (0.16)	88	0.021	11.12	2.40

^aExperimental error of $\pm 10\%$.**Figure 11.** Time-resolved decay of curcumin in 0.75 mM SB-16 solution with variation of temperature (a) and Arrhenius plots of $\ln(k_{nr})$ versus $1/T$ of curcumin in SB-16 micelle (b).

electrolytes, which decrease the CMC of SB-16 micelle leading to the higher partitioned of curcumin to micellar aggregates. The time-resolved experiments with the addition of NaCl to curcumin–SB16 micellar system have also been performed (Figure 10c). The results obtained are consistent with our steady state results. The average lifetime value of curcumin increased from 104 ps with components 79 (84%) and 236 (16%) ps to 137 ps with components 98 (77%) and 270 (23%). All the experimental data are gathered in Table 4. We have already mentioned that an opposite effect is observed on addition of anionic surfactant (SDS) to SB-16 micellar system. From the steady-state results it was clear that with gradual increase of SDS concentration the hydration of the palisade layer of the zwitterionic micelle (SB-16) increases, leading to the movement of the drug molecules from the palisade layer of the zwitterionic micelle to the bulk water. To confirm our steady state observation we measured the lifetime of curcumin in SB-16 micellar system with addition of SDS. The lifetime values are gather in Table 5 and depicted in Figure 10d. The average lifetime value of curcumin decreases from 104 ps with components 79 (84%) and 236 (16%) ps to 71 ps with components 56 (87%) and 174 (0.13%). This decrease in lifetime of curcumin with addition of SDS is an implication of the movement of the curcumin toward the bulk water. More specifically, we can say that, due to the movement of the curcumin toward the bulk water, ESIPT process, i.e., the main deactivation process of curcumin, increases causing a decrease in fluorescence lifetime.

To further understand the excited state dynamics of curcumin after partitioning into the micellar aggregates, it is necessary to calculate the radiative (k_r) and nonradiative (k_{nr}) decay rate constants. The required equations are given below:

$$k_r = \frac{\phi_f}{\tau_f} \quad (9)$$

$$k_{nr} = \frac{1}{\tau_f} - k_r \quad (10)$$

The calculated values are collected in Table 2. The change in the radiative decay rate is negligible with respect to nonradiative rate for all the cases mentioned above. From Table 2, it is evident that at 0.40 mM SB-16, the nonradiative rate constant of curcumin is $18.54 \times 10^9 s^{-1}$. Now, with gradual increase in the concentration of SB-16 the nonradiative rate constant is decreased to $9.30 \times 10^9 s^{-1}$ at a concentration of 0.75 mM. Thus, an enhancement in the fluorescence intensity and radiative lifetime (τ_f) of curcumin in the micellar aggregates can be assigned with reduction in the radiationless decay channels in these environments. Moreover, with addition of EmimHS to SB16 micellar system similar observation is found, i.e., the nonradiative rate constant again reduces from 9.30×10^9 to $6.91 \times 10^9 s^{-1}$ in the presence of 1.47 wt % EmimHS (Table 3). As the ESIPT process in curcumin has been considered to be a nonradiative process, the significant changes observed in the nonradiative rates reveal that excited-state intermolecular hydrogen-bonding between the curcumin and SB-16 significantly perturbed the excited state of the curcumin. However, the reverse effect is found upon addition of anionic surfactant (SDS), where the nonradiative rate constant increases from 9.30×10^9 to $13.84 \times 10^9 s^{-1}$, which is consistent with our steady state results, and could be explained by considering the movement of the curcumin toward bulk water. The measurements of lifetime with variation of temperature have also been performed. The lifetime values are listed in Table 6 and the representative decay profiles are shown in Figure 11a. With elevation of temperature from 288

to 308 K the nonradiative rate constant increases from 6.76×10^9 to $11.12 \times 10^9 \text{ s}^{-1}$. This increase in value can be attributed to the decrease in the numerical value of the quantum yield as well as the lifetime of curcumin. This phenomenon can be justified by considering the fact that at higher temperature the accessibility of water into zwitterionic micellar system increases as a result water-assisted nonradiative decay channels also increases. The temperature dependency experiments of the nonradiative decay further helps us to calculate the activation energy for these processes of curcumin in our investigated micellar system. Figure 11b shows the Arrhenius plot of $\ln(k_{\text{nr}})$ versus $1/T$ of curcumin in SB-16 micelles. The calculated value obtained from Figure 11b is 18.79 KJ/mol which is similar to literature values.^{31,75}

4. CONCLUSION

The present investigation deciphers the photophysics of a potent ESIPT molecule, curcumin, upon interaction with a zwitterionic micellar system (SB-16), and the work has also been extended to RTILs and anionic surfactant. From the scrutiny of steady state and time-resolved data, it is clear that the ESIPT process, the main photophysical process for deactivation of excited state, can be controlled within these organized assemblies. Close inspection of the emission spectra advocates for a greater degree of partitioning of the probe into zwitterionic micellar system. These results have also been well supported by the anisotropy data related to the rigidity imposed on curcumin. The fluorescence intensity of our investigated drug molecule, curcumin, as well as lifetime values, dramatically increases with increasing concentration of zwitterionic surfactant (SB-16); addition of anions with long chain (RTILs) leads us to the similar observation. The efficacy to reduce the ESIPT process depends upon the alkyl chain length of the RTILs; generally, the longer the chain length of the RTILs, the higher the efficiency to reduce the ESIPT process. However, the observation with addition of anionic surfactant (SDS) to the SB-16 micelle was completely reversed compared to RTILs. With gradual increase in the concentration of SDS, the migration of the curcumin molecules is observed toward the bulk water leading to hydration of the palisade layer of zwitterionic micelles. Furthermore, it has also been shown that the stability of curcumin drastically improved in our experimental systems.

AUTHOR INFORMATION

Corresponding Author

*E-mail: nilmoni@chem.iitkgp.ernet.in. Fax: 91-3222-255303.

Notes

The authors declare no competing financial interest.

ACKNOWLEDGMENTS

N.S. is thankful to Council of Scientific and Industrial Research (CSIR) for a generous research grant. C. B., J. K. are thankful to UGC; S. G., S. M. are thankful to CSIR; N. K. is thankful to IIT Kharagpur for research fellowships.

REFERENCES

- (1) Butler, M. S. The Role of Natural Product Chemistry in Drug Discovery. *J. Nat. Prod.* **2004**, *67*, 2141–53.
- (2) Newman, D. J.; Cragg, G. M. Natural Products as Sources of New Drugs Over the Last 25 years. *J. Nat. Prod.* **2007**, *70*, 461–77.
- (3) Sharma, R. A.; Gescher, A. J.; Steward, W. P. Curcumin: The Story so far. *Eur. J. Cancer* **2005**, *41*, 1955–1968.
- (4) Goel, A.; Kunnumakkara, A. B.; Aggarwal, B. B. Curcumin as “Curcumin”: From Kitchen to Clinic. *Biochem. Pharmacol.* **2008**, *75*, 787–809.
- (5) Sharma, O. P. Antioxidant Activity of Curcumin and Related Compounds. *Biochem. Pharmacol.* **1976**, *25*, 1811–1812.
- (6) Khar, A.; Ali, A. M.; Pardhasaradhi, B. V.; Begum, Z.; Anjum, R. Antitumor Activity of Curcumin is Mediated Through the Induction of Apoptosis in AK-5 tumor cells. *FEBS Lett.* **1999**, *445*, 165–168.
- (7) Chan, M. M.; Huang, H. I.; Fenton, M. R.; Fong, D. In Vivo Inhibition of Nitric Oxide Synthase Gene Expression by Curcumin, a Cancer Preventive Natural Product with Anti-inflammatory Properties. *Biochem. Pharmacol.* **1998**, *55*, 1955–1962.
- (8) Aggarwal, B. B.; Kumar, A.; Bharti, A. C. Anticancer Potential of Curcumin: Preclinical and Clinical Studies. *Anticancer Res.* **2003**, *23*, 363–398.
- (9) Anand, P.; Kunnumakkara, A. B.; Newman, R. A.; Aggarwal, B. B. Bioavailability of Curcumin: Problems and Promises. *Mol. Pharmacol.* **2007**, *4*, 807–818.
- (10) Maiti, K.; Mukherjee, K.; Gantait, A.; Saha, B. P.; Mukherjee, P. K. Curcumin-Phospholipid Complex: Preparation, Therapeutic Evaluation and Pharmacokinetic Study in Rats. *Int. J. Pharm.* **2007**, *330*, 155–163.
- (11) Tonnesen, H. H.; Karlsen, J.; Mostad, A. Structural Studies of Curcuminoids. I. The Crystal Structure of Curcumin. *Acta Chem. Scand., Ser. B* **1982**, *36*, 475–480.
- (12) Parmita, S. P.; Ramshankar, Y. V.; Suresh, S.; Guru, R. T. N. Redetermination of Curcumin: (1E,4Z,6E)-5-hydroxy-1,7-bis-(4-hydroxy-3-methoxy-phen-yl)hepta-1,4,6-trien-3-one. *Acta Crystallogr., Sect. E* **2007**, *63*, o860–o862.
- (13) Sun, Y. M.; Wang, R. X.; Yuan, S. L.; Lin, X. J.; Liu, C. B. Theoretical Study on the Antioxidant Activity of Curcumin. *Chinese J. Chem.* **2004**, *22*, 827–830.
- (14) Ghosh, R.; Mondal, J. A.; Palit, D. K. Ultrafast Dynamics of the Excited States of Curcumin in Solution. *J. Phys. Chem. B* **2010**, *114*, 12129–12143.
- (15) Saini, R. K.; Das, K. Picosecond Spectral Relaxation of Curcumin Excited State in a Binary Solvent Mixture of Toluene and Methanol. *J. Phys. Chem. B* **2012**, *116*, 10357–10363.
- (16) Balasubramanian, K. Molecular Orbital Basis for Yellow Curry Spice Curcumin's Prevention of Alzheimer's Disease. *J. Agric. Food Chem.* **2006**, *54*, 3512–3520.
- (17) Shen, L.; Ji, H. F.; Zhang, H. Y. A TD-DFT Study on Triplet Excited-State Properties of Curcumin and its Implications in Elucidating the Photosensitizing Mechanisms of the Pigment. *Chem. Phys. Lett.* **2005**, *409*, 300–303.
- (18) Shen, L.; Zhang, H. Y.; Ji, H. F. Successful Application of TD-DFT in Transient Absorption Spectra Assignment. *Org. Lett.* **2005**, *7*, 243–246.
- (19) Bonancía, P.; Vayá, I.; José Climent, M.; Gustavsson, T.; Markovitsi, D.; Jimenez, M. C.; Miranda, M. A. Excited-State Interactions in Diastereomeric Flurbiprofen–Thymine Dyads. *J. Phys. Chem. A* **2012**, *116*, 8807–8814.
- (20) Miannay, F. A.; Gustavsson, T.; Banyasz, A.; Markovitsi, D. Excited-State Dynamics of dGMP Measured by Steady-State and Femtosecond Fluorescence Spectroscopy. *J. Phys. Chem. A* **2010**, *114*, 3256–3263.
- (21) Akos Banyasz, A.; Douki, T.; Improt, R.; Gustavsson, T.; Onidas, D.; Vaya, I.; Perron, M.; Markovitsi, D. Electronic Excited States Responsible for Dimer Formation upon UV Absorption Directly by Thymine Strands: Joint Experimental and Theoretical Study. *J. Am. Chem. Soc.* **2012**, *134*, 14834–14845.
- (22) Jasim, F.; Ali, F. A Novel and Rapid Method for the Spectrofluorometric Determination of Curcumin in Curcumin Spices and Flavors. *Microchem. J.* **1992**, *46*, 209–214.
- (23) Zsila, F.; Bikadi, Z.; Simonyi, M. Molecular Basis of the Cotton effects Induced by the Binding of Curcumin to Human Serum Albumin. *Tetrahedron: Asymmetry* **2003**, *14*, 2433–2444.

- (24) Mandeville, J. S.; Froehlich, E.; Tajmir-Riahi, H. A. Study of Curcumin and Genistein Interactions with Human Serum Albumin. *J. Pharm. Biomed. Anal.* **2009**, *49*, 468–474.
- (25) Began, G.; Sudharshan, E.; Udaya, S. K.; Appu Rao, A. G. Interaction of Curcumin with Phosphatidylcholine: A Spectrofluorometric Study. *J. Agric. Food Chem.* **1999**, *47*, 4992–4997.
- (26) Chignell, C. F.; Bilski, P.; Reszka, K. J.; Motten, A. N.; Sik, R. H.; Dhal, T. A. Spectral and Photochemical Properties of Curcumin. *Photochem. Photobiol.* **1994**, *59*, 295–302.
- (27) Tonnesen, H. H.; Arrieta, A. F.; Lerner, D. Studies on Curcumin and Curcuminoids 0.24. Characterization of the Spectroscopic Properties of the Naturally-Occurring Curcuminoids and Selective Derivatives. *Pharmazie* **1995**, *50*, 689–693.
- (28) Khopde, S. M.; Priyadarsini, K. I.; Palit, D. K.; Mukherjee, T. Effect of Solvent on the Excited-State Photophysical Properties of Curcumin. *Photochem. Photobiol.* **2000**, *72*, 625–631.
- (29) Kapoor, S.; Priyadarsini, K. I. Protection of Radiation-Induced Protein Damage by Curcumin. *Biophys. Chem.* **2001**, *92*, 119–126.
- (30) Kunwar, A.; Barik, A.; Pandey, R.; Priyadarsini, K. I. Transport of Liposomal and Albumin Loaded Curcumin to Living Cells: an Absorption and Fluorescence Spectroscopic Study. *Biochim. Biophys. Acta* **2006**, *1760*, 1513–1520.
- (31) Erez, Y.; Presiado, I.; Gepshtein, R.; Huppert, D. Temperature Dependence of the Fluorescence Properties of Curcumin. *J. Phys. Chem. A* **2011**, *115*, 10962–10971.
- (32) Erez, Y.; Presiado, I.; Gepshtein, R.; Huppert, D. The Effect of a Mild Base on Curcumin in Methanol and Ethanol. *J. Phys. Chem. A* **2012**, *116*, 2039–2048.
- (33) Zhang, H. X.; Annunziata, O. Modulation of Drug Transport Properties by Multicomponent Diffusion in Surfactant Aqueous Solutions. *Langmuir* **2008**, *24*, 10680–10687.
- (34) Bhat, P. A.; Rather, G. M.; Dar, A. A. Effect of Surfactant Mixing on Partitioning of Model Hydrophobic Drug, Naproxen, Between Aqueous and Micellar Phases. *J. Phys. Chem. B* **2009**, *113*, 997–1006.
- (35) Gomez-Mendoza, M.; Nuin, E.; Andreu, I.; Marin, M. L.; Miranda, M. A. Photophysical Probes to Assess the Potential of Cholic Acid Aggregates as Drug Carriers. *J. Phys. Chem. B* **2012**, *116*, 10213–10218.
- (36) Rohacova, J.; Marin, M. L.; Martinez-Romero, A.; Diaz, L.; O'Connor, J. E.; Gomez-Lechon, M. J.; Donato, M. T.; Castell, J. V.; Miranda, M. A. Fluorescent Benzofuran–Cholic Acid Conjugates for In Vitro Assessment of Bile Acid Uptake and Its Modulation by Drugs. *ChemMedChem* **2009**, *4*, 466–472.
- (37) Adhikary, R.; Carlson, P. J.; Kee, T. W.; Petrich, J. W. Excited-State Intramolecular Hydrogen Atom Transfer of Curcumin in Surfactant Micelles. *J. Phys. Chem. B* **2010**, *114*, 2997–3004.
- (38) Leung, M. H. M.; Colangelo, H.; Kee, T. W. Encapsulation of Curcumin in Cationic Micelles Suppresses Alkaline Hydrolysis. *Langmuir* **2008**, *24*, 5672–5675.
- (39) Wang, D.; Veena, M. S.; Stevenson, K.; Tang, C.; Ho, B.; Suh, J. D.; Duarte, V. M.; Faull, K. F.; Mehta, K.; Srivatsan, E. S.; Wang, M. B. Liposome-Encapsulated Curcumin Suppresses Growth of Head and Neck Squamous Cell Carcinoma In Vitro and In Xenografts Through the Inhibition of Nuclear Factor κ B by an AKT-Independent Pathway. *Clin. Cancer Res.* **2008**, *14*, 6228–6236.
- (40) Gupta, V.; Aseh, A.; Rios, C. N.; Aggarwal, B. B.; Mathur, A. B. Fabrication and Characterization of Silk Fibroin-Derived Curcumin Nanoparticles for Cancer Therapy. *Int. J. Nanomed.* **2009**, *4*, 115–122.
- (41) Lemos, M. A.; Hungerford, G. The Binding of Curcuma Longa Extract with Bovine Serum Albumin Monitored via Time-Resolved Fluorescence. *Photochem. Photobiol.* **2013**, *89*, 1071–1078.
- (42) Das, R. K.; Kasoju, N.; Bora, U. Encapsulation of Curcumin in Alginate-Chitosan-Pluronic Composite Nanoparticles for Delivery to Cancer Cells. *Nanomedicine* **2010**, *6*, 153–160.
- (43) Maiti, K.; Mukherjee, K.; Gantait, A.; Saha, B. P.; Mukherjee, P. K. Curcumin-Phospholipid Complex: Preparation, Therapeutic Evaluation and Pharmacokinetic Study in Rats. *Int. J. Pharm.* **2007**, *330*, 155–163.
- (44) Yallapu, M. M.; Jaggi, M.; Chauhan, S. C. Poly(β -cyclodextrin)/Curcumin Self-Assembly: A Novel Approach to Improve Curcumin Delivery and its Therapeutic Efficacy in Prostate Cancer Cells. *Macromol. Biosci.* **2010**, *10*, 1141–1151.
- (45) *Ionic Liquids: Industrial Applications for Green Chemistry*; Rogers, R. D., Seddon, K. R., Eds.; ACS Symposium Series 818; American Chemical Society: Washington, DC, 2002.
- (46) *Ionic Liquids III: Fundamentals, Challenges, and Opportunities*; Rogers, R. D., Seddon, K. R., Eds.; ACS Symposium Series 901; American Chemical Society: Washington, DC, 2005.
- (47) Patra, D.; Barakat, C. Unique Role of Ionic Liquid [bmin][BF₄] During Curcumin–Surfactant Association and Micellization of Cationic, Anionic and Non-ionic Surfactant Solutions. *Spectrochim. Acta, Part A* **2011**, *79*, 1823–1828.
- (48) Hallett, J. P.; Welton, T. Room-Temperature Ionic Liquids: Solvents for Synthesis and Catalysis. 2. *Chem. Rev.* **2011**, *111*, 3508–3576.
- (49) Behera, K.; Pandey, S. Concentration-Dependent Dual Behavior of Hydrophilic Ionic Liquid in Changing Properties of Aqueous Sodium Dodecyl Sulfate. *J. Phys. Chem. B* **2007**, *111*, 13307–13315.
- (50) Behera, K.; Pandey, D. M.; Porel, M.; Pandey, S. Unique Role of Hydrophilic Ionic Liquid in Modifying Properties of Aqueous Triton X-100. *J. Chem. Phys.* **2007**, *127*, 184501–184510.
- (51) Rao, V. G.; Ghatak, C.; Ghosh, S.; Mandal, S.; Sarkar, N. The Chameleon-Like Nature of Zwitterionic Micelles: The Effect of Ionic Liquid Addition on the Properties of Aqueous Sulfobetaine Micelles. *ChemPhysChem* **2012**, *13*, 1–10.
- (52) Banerjee, C.; Mandal, S.; Ghosh, S.; Rao, V. G.; Sarkar, N. Tuning the Probe Location on Zwitterionic Micellar System with Variation of pH and Addition of Surfactants with Different Alkyl Chains: Solvent and Rotational Relaxation Studies. *J. Phys. Chem. B* **2012**, *116*, 11313–11322.
- (53) Sarkar, A.; Trivedi, S.; Pandey, S. Polymer Molecular Weight-Dependent Unusual Fluorescence Probe Behavior within 1-Butyl-3-Methylimidazolium Hexafluorophosphate+poly(ethylene glycol). *J. Phys. Chem. B* **2009**, *113*, 7606–7614.
- (54) Rai, R.; Baker, A. G.; Behera, K.; Mohanty, P.; Kurur, D. N.; Pandey, S. Ionic Liquid-Induced Unprecedented Size Enhancement of Aggregates within Aqueous Sodium Dodecylbenzene Sulfonate. *Langmuir* **2010**, *26*, 17821–17826.
- (55) Behera, K.; Pandey, S. Ionic Liquid Induced Changes in the Properties of Aqueous Zwitterionic Surfactant Solution. *Langmuir* **2008**, *24*, 6462–6469.
- (56) Lakowicz, J. R. Principles of Fluorescence Spectroscopy; Plenum: New York, 1999; Vol. 2.
- (57) Hazra, P.; Chakrabarty, D.; Sarkar, N. Solvation Dynamics of Coumarin 153 in Aqueous and Non-aqueous Reverse Micelles. *Chem. Phys. Lett.* **2003**, *371*, 553–562.
- (58) Jones, G. II; Jackson, W. R.; Choi, C.-Y.; Bergmark, W. R. Solvent Effect on Emission Yield and Lifetime of Coumarin Laser Dyes: Requirements for Rotatory Decay Mechanism. *J. Phys. Chem.* **1985**, *89*, 294–300.
- (59) Zsila, F.; Bikadi, Z.; Simonyi, M. Circular Dichroism Spectroscopic Studies Reveal pH Dependent Binding of Curcumin in the Minor Groove of Natural and Synthetic Nucleic Acids. *Org. Biomol. Chem.* **2004**, *2*, 2902–2910.
- (60) Ke, D.; Wang, X.; Yang, Q.; Niu, Y.; Chai, S.; Chen, Z.; An, X.; Shen, W. Spectrometric Study on the Interaction of Dodecyltrimethylammonium Bromide with Curcumin. *Langmuir* **2011**, *27*, 14112–14117.
- (61) Adhikary, R.; Mukherjee, P.; Kee, T. W.; Petrich, J. W. Excited-State Intramolecular Hydrogen Atom Transfer and Solvation Dynamics of the Medicinal Pigment Curcumin. *J. Phys. Chem. B* **2009**, *113*, 5255–5261.
- (62) Shutava, T. G.; Balkundi, S. S.; Vangala, P.; Steffan, J. J.; Bigelow, R. L.; Cardelli, J. A.; et al. Layer-by-Layer-Coated Gelatin Nanoparticles as a Vehicle for Delivery of Natural Polyphenols. *ACS Nano* **2009**, *3*, 1877–1885.

- (63) Shieh, Y. A.; Yang, S. J.; Wei, M. F.; Shieh, M. J. Aptamer-Based Tumor-Targeted Drug Delivery for Photodynamic Therapy. *ACS Nano* **2010**, *4*, 1433–42.
- (64) Wang, X.; Yang, L.; Chen, Z.; Shin, D. M. Application of Nanotechnology in Cancer Therapy and Imaging. *CA Cancer J. Clin.* **2008**, *58*, 97–110.
- (65) Rodrigues, C.; Gamberio, P.; Reis, S.; Lima, J. L. F. C.; Castro, B. D. Interaction of Grepafloxacin with Large Unilamellar Liposomes: Partition and Fluorescence Studies Reveal the Importance of Charge Interactions. *Langmuir* **2002**, *18*, 10231–10236.
- (66) Paul, B. K.; Samanta, A.; Guchhait, N. Modulation of Excited-State Intramolecular Proton Transfer Reaction of 1-hydroxy-2-naphthaldehyde in Different Supramolecular Assemblies. *Langmuir* **2010**, *26*, 3214–3224.
- (67) Mandal, S.; Rao, V. G.; Ghatak, C.; Pramanik, R.; Sarkar, S.; Sarkar, N. Photophysics and Photodynamics of 1'-Hydroxy-2'-acetonaphthone (HAN) in Micelles and Nonionic Surfactants Forming Vesicles: A Comparative Study of Different Microenvironments of Surfactant Assemblies. *J. Phys. Chem. B* **2011**, *115*, 12108–12119.
- (68) Mandal, S.; Ghosh, S.; Banik, D.; Banerjee, C.; Kuchlyan, J.; Sarkar, N. An Investigation into the Effect of the Structure of Bile Salt Aggregates on the Binding Interactions and ESIHT Dynamics of Curcumin: A Photophysical Approach To Probe Bile Salt Aggregates as a Potential Drug Carrier. *J. Phys. Chem. B* **2013**, *117*, 13795–13807.
- (69) Ghatak, C.; Rao, V. G.; Mandal, S.; Ghosh, S.; Sarkar, N. An Understanding of the Modulation of Photophysical Properties of Curcumin Inside a Micelle Formed by an Ionic Liquid: A New Possibility of Tunable Drug Delivery System. *J. Phys. Chem. B* **2012**, *116*, 3369–3379.
- (70) Banerjee, C.; Ghatak, C.; Mandal, S.; Ghosh, S.; Kuchlyan, J.; Sarkar, N. Curcumin in Reverse Micelle: An Example to Control Excited-State Intramolecular Proton Transfer (ESIPT) in Confined Media. *J. Phys. Chem. B* **2013**, *117*, 6906–6916.
- (71) Almgren, M.; Grieser, F.; Thomas, J. K. Dynamic and Static Aspects of Solubilization of Neutral Arenes in Ionic Micellar Solutions. *J. Am. Chem. Soc.* **1979**, *101*, 279–291.
- (72) Harada, T.; Pham, D.-T.; Leung, M. H. M.; Ngo, H. T.; Lincoln, S. F.; Easton, C. J.; Kee, T. W. Cooperative Binding and Stabilization of the Medicinal Pigment Curcumin by Diamide Linked γ -Cyclodextrin Dimers: A Spectroscopic Characterization. *J. Phys. Chem. B* **2011**, *115*, 1268–1274.
- (73) Leung, M. H. M.; Kee, T. W. Effective Stabilization of Curcumin by Association to Plasma Proteins: Human Serum Albumin and Fibrinogen. *Langmuir* **2009**, *25*, 5773–5777.
- (74) Patra, D.; Barakat, C.; Tafech, R. M. Study on Effect of Lipophilic Curcumin on Sub-Domain IIA Site of Human Serum Albumin During Unfolded and Refolded States: A Synchronous Fluorescence Spectroscopic Study. *Colloids Surf., B* **2012**, *94*, 354–361.
- (75) Mandal, S.; Banerjee, C.; Ghosh, S.; Kuchlyan, J.; Sarkar, N. Modulation of the Photophysical Properties of Curcumin in Non-ionic Surfactant (Tween-20) Forming Micelles and Niosomes: A Comparative Study of Different Microenvironments. *J. Phys. Chem. B* **2013**, *117*, 6957–6968.
- (76) Gou, M.; Men, K.; Shi, S. H.; Xiang, L. M.; Zhang, J.; Song, J.; Long, L. J.; Wan, Y.; Luo, F.; Zhao, X.; Qian, Y. Z. Curcumin-Loaded Biodegradable Polymeric Micelles for Colon Cancer Therapy In Vitro and In Vivo. *Nanoscale* **2011**, *3*, 1558–1567.
- (77) Zhang, Y. Z.; Dai, J.; Zhang, X. P.; Yang, X.; Liu, Y. Studies of the Interaction Between Sudan I and Bovine Serum Albumin by Spectroscopic Methods. *J. Mol. Struct.* **2008**, *888*, 152–159.
- (78) Ross, P. D.; Subramanian, S. Thermodynamics of Protein Association Reactions: Forces Contributing to Stability. *Biochemistry* **1981**, *20*, 3096–3102.
- (79) Nardo, L.; Paderno, R.; Andreoni, A.; Masson, M.; Haukvik, T.; Tønnesen, H. H. Role of H-bond Formation in the Photoreactivity of Curcumin. *Spectroscopy* **2008**, *22*, 187–198.
- (80) Nardo, L.; Andreoni, A.; Masson, M.; Haukvik, T.; Tønnesen, H. H. Studies on Curcumin and Curcuminoids. XXXIX. Photophysical Properties of Bisdemethoxycurcumin. *J. Fluoresc.* **2011**, *21*, 627–635.
- (81) Schwartz, B. J.; Peteanu, L. A.; Harris, C. B. Direct Observation of Fast Proton Transfer: Femtosecond Photophysics of 3-hydroxyflavone. *J. Phys. Chem.* **1992**, *96*, 3591–3598.